An Effective Approach to Predict Performances of High Speed BLDC Motors in Hard Disk Drives

Quan Jiang
Data Storage Institute
5, Engineering Drive 1
Singapore 117608
SINGAPORE
JIANG_Quan@dsi.A-Star.edu.sg

Chao Bi
Data Storage Institute
5, Engineering Drive 1
Singapore 117608
SINGAPORE
BI_Chao@dsi.A-Star.edu.sg

Abdullah Al Mamun
Dept. of Electrical & Computer Engg.
National University of Singapore
10 Kent Ridge Crescent
SINGAPORE 119260
eleaam@nus.edu.sg

***Abstract* – As the speed of the BLDC motors in hard disk drives has been increased from 3,600 rpm to 15,000 rpm, the phase commutation of the motor and the MOSFET switches of inverter influence the spindle motor performances obviously, for examples, the torque ripple and efficiency of the motor. In this paper, an effective approach of BLDC spindle motor system is presented to predict the performance of BLDC motors accurately. Both the characteristics of the spindle motor and MOSFET switches of the inverter can be taken into account in the simulation. The experimental results confirmed the effectiveness of the proposed method.**

I. INTRODUCTION

Spindle motors are driving to high speed and compact size in hard disk drive (HDD) area, particularly those in the servers and consumer portable appliances. The recording density of commercial HDDs has been increased 25 million times since the first HDD was invented and will reach 200 Gb/in^2 in near future [1]. In order to read and write the huge data with fast rate, the spin-speed of the spindle motors in HDD has been gradually increased from 3,600 rpm to 15,000 rpm since 1991. Soon the spin-speed will reach 20,000 rpm or even higher. As the spin-speed increases, the commutation during BLDC operation mode will obviously influence the performances of the motor, e.g., the torque ripple and efficiency of the motor, and such influences should be taken into account in the analysis and applications of the spindle motors [2]. Because HDD power supply voltages may be as low as 3.3V (1.8" and 1" HDDs), the voltage-drops of power MOSFETs and freewheeling diodes also must be considered for estimating accurately the performances of spindle motors.

Many investigations have been done to model and predict the performances of BLDC motors [3]. But the most of these models, calculations and analyses are based on state-variable model or Fourier series [3,4]. They usually adopt the numerical time-step integration approach and do not take account of the voltage drops of switching-on switches and the freewheeling diodes in the power inverters. Those methods are generally time-consuming in the analysis and difficult to be used to optimize the motor design parameters and control variables. The neglects of voltage-drops on the switches and freewheeling diodes, i.e., assuming them to be ideal devices with zero voltage drop, maybe be acceptable for high voltage BLDC motor drives, but it will cause obvious errors in calculating the performances of spindle motors in HDD, which supply voltages is no higher than 12V and may be as low as 3.3V in micro-HDD drives.

In this paper, a mathematic model of BLDC spindle motor drive system will be presented for describing the normal and commutating transient operation. The model is based on directly analytical solutions. Using the model, both the characteristics of the spindle motor and MOSFET switches of the inverters can be considered. Through the suggested procedure, the optimal control of BLDC spindle motor drives can be further explored to make the torque ripple be minimum or efficiency be maximum. During the analyses, a spindle motor drive designed for 3.5" hard disk drives will be used as an example to demonstrate the application of the proposed model.

II. MATHEMATICAL MODEL OF SPINDLE MOTORS

Since HDDs are very compact in size and sensitive to the leakage magnetic field of the spindle motor, almost all spindle motors used in HDDs are three-phase permanent magnetic motor which is position sensorless and operates in BLDC mode with sinusoidal back EMFs, as shown in Fig. 1 and 2. In Fig. 1, an adjustable DC/DC voltage regulator is employed to realize high accurate speed control in constant voltage BLDC mode instead of PMM chopping control.

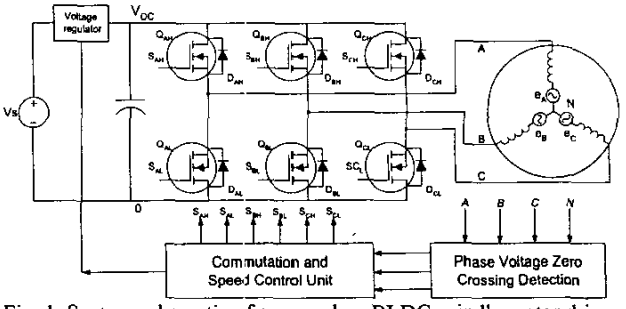

Fig. 1. System schematic of a sensorless BLDC spindle motor drive.

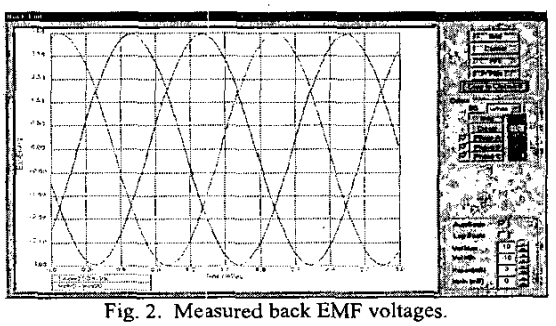

Fig. 2. Measured back EMF voltages.

In general, a permanent magnet (PM) motor with sinusoidal back EMF waveforms can be modelled by the following equations:

$$\begin{cases} e_A(\theta) = k_e \omega_r \sin(\theta) \\ e_B(\theta) = e_A(\theta - \frac{2}{3}\pi) = k_e \omega_r \sin(\theta - \frac{2}{3}\pi) \\ e_C(\theta) = e_A(\theta - \frac{4}{3}\pi) = k_e \omega_r \sin(\theta - \frac{4}{3}\pi) \end{cases}, \quad (1)$$

$$i_A + i_B + i_C = 0, \quad (2)$$

$$\begin{bmatrix} V_A \\ V_B \\ V_C \end{bmatrix} = \begin{bmatrix} e_A \\ e_B \\ e_C \end{bmatrix} + \begin{bmatrix} R_A & & \\ & R_B & \\ & & R_C \end{bmatrix} \begin{bmatrix} i_A \\ i_B \\ i_C \end{bmatrix} + \begin{bmatrix} L_{AA} & M_{AB} & M_{AC} \\ M_{AB} & L_{BB} & M_{BC} \\ M_{AC} & M_{BC} & L_{CC} \end{bmatrix} \frac{d}{dt} \begin{bmatrix} i_A \\ i_B \\ i_C \end{bmatrix} + \begin{bmatrix} V_n \\ V_n \\ V_n \end{bmatrix}, \quad (3)$$

$$T_{em} = \frac{p_p}{\omega_r}(e_A \times i_A + e_B \times i_B + e_C \times i_C), \quad (4)$$

$$\frac{J}{p_p}\frac{d\omega_r}{dt} = T_{em} + T_{cogging} - T_f - T_{load} \quad (5)$$

where V_A, V_B, and V_C are terminal voltages of the motor, V_n is its neutral point voltage, i_A, i_B and i_C are phase currents, e_A, e_B, and e_C are phase back EMFs, R_A, R_B, and R_C are phase resistances, L_{AA}, L_{BB}, and L_{CC} are phase self inductances, M_{AB}, M_{BC} and M_{AC} are phase to phase mutual inductances, p_p is the number of pole-pairs, T_{em} is the electromagnetic torque produced by the phase currents, $T_{cogging}$ is the cogging torque, J is the system inertia, ω_r is the electrical angle speed of rotor, θ is the rotor position in electric degree relative to the stator, T_f is the friction torque, and T_{load} is the load torque.

Almost all the spindle motors used in HDDs utilize fractional armature windings for realizing compact size and multi magnetic poles. After structure optimization, this kind of armature windings can reduce the cogging torque to a very small value. Therefore, in this paper, the effects of the cogging torque will not be taken account in the analysis.

Assumed that the motor is three-phase symmetric and the inductances are independent on the rotor position, the above equations of the motor at the constant mechanical speed n rpm can be simplified and rewritten as,

$$\omega_r = p_p \frac{2\pi}{60} n, \quad (6)$$

$$V_n = \frac{1}{3}(V_A + V_B + V_C), \quad (7)$$

$$\begin{cases} \omega_r L_e \frac{di_A}{d\theta} + Ri_A = V_A - V_n - e_A = V_{An} - e_A \\ \omega_r L_e \frac{di_B}{d\theta} + Ri_B = V_B - V_n - e_B = V_{Bn} - e_B \\ \omega_r L_e \frac{di_C}{d\theta} + Ri_C = V_C - V_n - e_C = V_{Cn} - e_C \end{cases}, \quad (8)$$

$$T_{out} = \frac{p_p}{\omega_r}(e_A \times i_A + e_B \times i_B + e_C \times i_C) - T_f, \quad (9)$$

where $R = R_A = R_B = R_C$, $M = M_{AB} = M_{BC} = M_{CA}$, $L_s = L_{AA} = L_{BB} = L_{CC}$, $L_e = L_s - M$, V_{An}, V_{Bn} and V_{Cn} are their phase voltages and T_{out} is the output torque of the motor.

When a spindle motor operates in a natural commutating BLDC mode, the switches and diodes will operate in sequence as shown in Table I. The operating periods can be classified into two categories, i.e., normal two-phase conducting periods and phase-shifting commutating periods. In Table I, the commutating period is supposed to last δ_C/ω_r seconds.

During period 1, when MOSFET Q_{CH} and Q_{BL} are switched on in Fig. 3, the terminal voltages and phase currents can be expressed as,

$$V_A = e_A + V_n, V_B = -i_B r_{DS} \text{ and } V_C = V_{DC} - i_C r_{DS}, \quad (10)$$

$$i_A = 0,\ i_B = -i_s \text{ and } i_C = i_s, \quad (11)$$

where r_{DS} is on-resistance of MOSFET switches. From (7) and (10), the neutral point voltage is obtained as,

$$V_n = \frac{1}{2}(V_{DC} + e_A). \quad (12)$$

Combining (8), (10) and (11), the following equation can be gotten,

$$\omega_r L_e \frac{di_S}{d\theta} + Ri_S = \frac{1}{2}(V_C - V_B - e_C + e_B)$$
$$= \frac{1}{2}(V_{DC} - 2r_{DS} i_S) + \frac{\sqrt{3}}{2} k_e \omega_r \sin(\theta - \frac{\pi}{2})$$

i.e.,

$$\omega_r L_e \frac{di_S}{d\theta} + (R + r_{DS}) i_S = \frac{1}{2}\left[V_{DC} + \sqrt{3} k_e \omega_r \sin(\theta - \frac{\pi}{2})\right]. \quad (13)$$

TABLE I
BLDC OPERATING PERIODS

Periods	1	C12	2	C23	3	C34
	$(-\frac{\pi}{6}+\delta_C, \frac{\pi}{6})$	$(\frac{\pi}{6}, \frac{\pi}{6}+\delta_C)$	$(\frac{\pi}{6}+\delta_C, \frac{\pi}{2})$	$(\frac{\pi}{2}, \frac{\pi}{2}+\delta_C)$	$(\frac{\pi}{2}+\delta_C, \frac{5\pi}{6})$	$(\frac{5\pi}{6}, \frac{5\pi}{6}+\delta_C)$
"On" devices	Q_{CH}, Q_{BL}	Q_{AH}, Q_{BL}, D_{CL}	Q_{AH}, Q_{BL}	Q_{AH}, Q_{CL}, D_{BH}	Q_{AH}, Q_{CL}	Q_{BH}, Q_{CL}, D_{AL}
Periods	4	C45	5	C56	6	C61
	$(\frac{5\pi}{6}+\delta_C, \frac{7\pi}{6})$	$(\frac{7\pi}{6}, \frac{7\pi}{6}+\delta_C)$	$(\frac{7\pi}{6}+\delta_C, \frac{3\pi}{2})$	$(\frac{3\pi}{2}, \frac{3\pi}{2}+\delta_C)$	$(\frac{3\pi}{2}+\delta_C, \frac{11}{6}\pi)$	$(\frac{11}{6}\pi, -\frac{\pi}{6}+\delta_C)$
"On" devices	Q_{BH}, Q_{CL}	Q_{BH}, Q_{AL}, D_{CH}	Q_{BH}, Q_{AL}	Q_{CH}, Q_{AL}, D_{BL}	Q_{CH}, Q_{AL}	Q_{CH}, Q_{BL}, D_{AH}

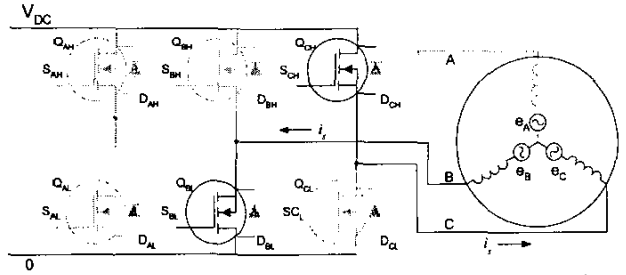

Fig. 3. Normal operating status of inverter during period 1

Solve (13) to find the current i_S,

$$i_S = [i_{S0} - \frac{V_{DC}}{2R_e} + \frac{\sqrt{3}k_e\omega_r}{2Z_e}\sin(\frac{2\pi}{3} - \delta_C + \alpha)]e^{-\frac{R_e}{\omega_r L_e}(\theta + \frac{\pi}{6} - \delta_C)} + \frac{V_{DC}}{2R_e} + \frac{\sqrt{3}k_e\omega_r}{2Z_e}\sin(\theta - \alpha - \frac{\pi}{2}), \quad (14)$$

where i_{S0} is the initial current of the normal conducting period, $R_e = R + r_{DS}$, $Z_e = \sqrt{(\omega_r L_e)^2 + R_e^2}$ and $\alpha = \tan^{-1}(\omega_r L_e / R_e)$.

Therefore, three phase currents during period 1 can be analytically and accurately expressed through (11) and (14).

When the rotor reaches position $\pi/6$, the commutation form phase C to phase A will happen and last until phase current i_C be reduced to zero. At the beginning moment of the period, i.e., $\theta = \pi/6$, the currents i_C and i_B can be determined by the following formula:

$$i_{C1} = -i_{B1} = i_{S1} = [i_{S0} - \frac{V_{DC}}{2R_e} + \frac{\sqrt{3}k_e\omega_r}{2Z_e}\sin(\frac{2\pi}{3} - \delta_C + \alpha)]e^{-\frac{R_e}{\omega_r L_e}(\frac{\pi}{3} - \delta_C)} + \frac{V_{DC}}{2R_e} - \frac{\sqrt{3}k_e\omega_r}{2Z_e}\sin(\alpha + \frac{\pi}{3}). \quad (15)$$

During this commutating transient period C12 shown in Fig. 4, switches Q_{AH} and Q_{BL} as well as freewheeling diode D_{CL} are on and the other switches are off. Then the terminal voltages and the neutral point voltage can be expressed as,

$$V_A = V_{DC} - r_{DS}i_A,\ V_B = -i_B r_{DS} \text{ and } V_C = -V_F, \quad (16)$$

$$V_n = \frac{1}{3}(V_{DC} - r_{DS}i_A - r_{DS}i_B - V_F) = \frac{1}{3}(V_{DC} + r_{DS}i_C - V_F), \quad (17)$$

where V_F is the voltage drop of the MOSFET anti-parallel diode during freewheeling. Combining (8) and (17) as well as the relative back EMFs in (1), the following equations are obtained:

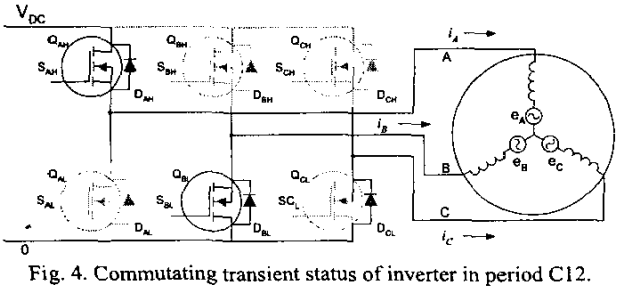

Fig. 4. Commutating transient status of inverter in period C12.

$$\omega_r L_e \frac{di_A}{d\theta} + R_e i_A = \frac{2}{3}V_{DC} + \frac{1}{3}V_F - k_e\omega_r\sin(\theta) - \frac{1}{3}r_{DS}i_C, \quad (18)$$

$$\omega_r L_e \frac{di_B}{d\theta} + R_e i_B = -\frac{1}{3}V_{DC} + \frac{1}{3}V_F - k_e\omega_r\sin(\theta - \frac{2\pi}{3}) - \frac{1}{3}r_{DS}i_C, \quad (19)$$

$$\omega_r L_e \frac{di_C}{d\theta} + R_e' i_C = -\frac{1}{3}V_{DC} - \frac{2}{3}V_F - k_e\omega_r\sin(\theta - \frac{4\pi}{3}), \quad (20)$$

where $R_e' = R + r_{DS}/3$. Solving (20), the phase C current i_C is:

$$i_C = \left[i_{S1} + \frac{V_{DC} + 2V_F}{3R_e'} + \frac{k_e\omega_r}{Z_e'}\sin(\frac{\pi}{6} + \alpha')\right]e^{-\frac{R_e'}{\omega_r L_e}(\theta - \frac{\pi}{6})} - \frac{V_{DC} + 2V_F}{3R_e'} + \frac{k_e\omega_r}{Z_e'}\sin(\theta - \frac{\pi}{3} - \alpha'), \quad (21)$$

where $Z_e' = \sqrt{(\omega_r L_e)^2 + R_e'^2}$ and $\alpha' = \tan^{-1}\frac{\omega_r L_e}{R_e'}$.

Replacing i_C in (18) with (21), the phase A current i_A can be solved as,

$$i_A = \frac{1}{3R_e}\left[2V_{DC} + V_F + \frac{r_{DS}}{3R_e'}(V_{DC} + 2V_F)\right]\left(1 - e^{-\frac{R_e}{\omega_r L_e}(\theta - \frac{\pi}{6})}\right) - \frac{k_c k_e\omega_r}{Z_e}\left(\sin(\theta - \alpha - \zeta) - \sin(\frac{\pi}{6} - \alpha - \zeta)e^{-\frac{R_e}{\omega_r L_e}(\theta - \frac{\pi}{6})}\right) + \frac{1}{2}\left[i_{S1} + \frac{V_{DC} + 2V_F}{3R_e'} + \frac{k_e\omega_r}{Z_e'}\sin(\frac{\pi}{6} + \alpha')\right]\left(e^{-\frac{R_e'}{\omega_r L_e}(\theta - \frac{\pi}{6})} - e^{-\frac{R_e}{\omega_r L_e}(\theta - \frac{\pi}{6})}\right), \quad (22)$$

where $k_c = \sqrt{\left[1 + \frac{r_{DS}}{3Z_e'}\cos(\frac{\pi}{3} + \alpha')\right]^2 + \left[\frac{r_{DS}}{3Z_e'}\sin(\frac{\pi}{3} + \alpha')\right]^2}$ and

$$\zeta = \tan^{-1}\frac{r_{DS}\sin(\frac{\pi}{3} + \alpha')}{3Z_e' + r_{DS}\cos(\frac{\pi}{3} + \alpha')}.$$

After currents i_C and i_A are available, the phase current i_B can be obtained by the following equation,

$$i_B(\theta) = -i_A(\theta) - i_C(\theta). \quad (23)$$

The commutating transient period of ($\pi/6$, $\pi/6+\delta_C$) will last until current i_C in (21) is reduced to zero. That is,

$$i_C(\frac{\pi}{6} + \delta_c) = 0 \quad (24)$$

$$i_A(\frac{\pi}{6} + \delta_c) = -i_B(\frac{\pi}{6} + \delta_c) = i_{S0}. \quad (25)$$

From (11), (14), (15), (21), (22) and (23), all three phase currents during normal operation and commutating periods can be accurately calculated and the correspondent torque can be obtained through (9). The effective electromagnetic torque and output torque can be expressed as following:

$$\overline{T}_{em} = \frac{3}{\pi}\int_{\frac{\pi}{6}+\delta_C}^{\frac{\pi}{6}+\delta_C} T_{em}(\theta)d\theta = \frac{3p_p}{\pi\omega_r}\left[\int_{\frac{\pi}{6}+\delta_C}^{\frac{\pi}{6}} (e_B i_B + e_C i_C)d\theta + \int_{\frac{\pi}{6}}^{\frac{\pi}{6}+\delta_C} (e_A i_A + e_B i_B + e_C i_C)d\theta\right]$$

and $\overline{T}_{out} = \overline{T}_{em} - T_f$. (26)

These equations are results during two particular periods, i.e., conduction period ($-\pi/6+\delta_C$, $\pi/6$) and commutating period ($\pi/6$, $\pi/6+\delta_C$). They are typical normal operation period and commutating period and the remained periods are same except the different phases as shown in Table I. It is easy to get their currents through the similar process as above.

One important feature of the above mathematical model and solution is that the characteristics of the inverter and its switches are taken into account through the MOSFET on-resistance r_{DS} and the freewheeling diode forward voltage drop V_F. Therefore, the power consumption of the inverter can also be accurately calculated. Based on the above model, the performances of both the BLDC motor and inverter can be accurately and analytically predicted in currents, output torque, torque ripple, input power, efficiency, RMS currents of switching devices and copper losses.

III. THE PROCEDURE TO PREDICT THE CURRENTS AND TOQURES

For introducing clearly the approach presented, a fluid dynamic bearing (FDB) spindle motor for 3.5" hard disk is instantiated and simulated based on the proposed mathematical model. The main parameters of the spindle motor and MOSFETs are shown in Table II. After all key parameters are known, the first step is to determine the motor speed and output torque. Secondly, the DC link voltage, V_{DC}, should be initialized and it is usually estimated about two times of amplitude value of phase back EMF at the specific speed as follows:

$$V_{DC}^{(0)} \approx 2k_e\omega_r. \quad (27)$$

Thirdly, starting with mean DC link current as initial current $i_{S0}^{(0)}$ of the two phase conduction period and zero commutating time $\delta_C^{(0)}$, i.e.,

$$i_{S0}^{(0)} \approx \frac{\omega_r \overline{T}_{out}}{p_p V_{DC}^{(0)}} = \frac{\omega_r}{p_p}\frac{1}{2k_e\omega_r}\overline{T}_{out} = \frac{\overline{T}_{out}}{2p_pk_e} \text{ and } \delta_C^{(0)} = 0,$$

the initial current $i_{S1}^{(0)}$ can be easily obtained through (15). Then, fourthly, the commutating time $\delta_C^{(1)}$ can be obtained by solving (21) and (24) with Newton iteration method since (21) is a super non-linear equation. Finally, the initial conduction current $i_{S0}^{(1)}$ of the new cycle can be obtained through (22) and (25). In this way, an operation cycle (two-phase conduction and commutation) is studied. Then the current at the end of the last cycle is taken as initial value of new cycle and so on until (25) is satisfied. It means that

$$\frac{|i_{S0}^{(k+1)} - i_{S0}^{(k)}|}{i_{S0}^{(k)}} \le \varepsilon,$$

where ε is the error limitation and can be set as small as necessary. After the initial currents and commutating time are obtained, the mean output torque can be calculated through (26) and the DC link voltage V_{DC} should be adjusted according to the difference between the required output torque and the calculated value. If the latter is larger, the DC link voltage should be reduced and other vice versa. The above detailed procedure is drawn in Fig. 5.

Through the suggested procedure, the input currents and the output torque of the motor in one typical cycle can be calculated. The initial and convergence values of the key variables during the steady-state simulation are listed in Table III. Fig. 6 and 7 display the simulated waveforms of three phase currents and torques. Fig. 8 and 9 shows the experimental waveforms of currents and torque. Comparing the calculated currents and torque with and experimental ones, it is clear that the accuracy of the proposed mathematic

TABLE II
MAIN PARAMETERS OF A 3.5" HDD FDB SPINDLE MOTOR

Name	Symbol	Value	Units
Rated speed	n	5400	rpm
Mean output torque	T_{out}	1.768	mNm
Friction torque	T_f	0.110	mNm
Pole pairs	p_p	6	
Phase resistance	R	2.98	Ω
Back EMF constant	k_e	1.166	mV/rad/s
Equivalent inductance	L_e	1.08	mH
MOSFET on-resistance	r_{DS}	2.00	Ω
Freewheeling diode voltage drop	V_F	0.67	V

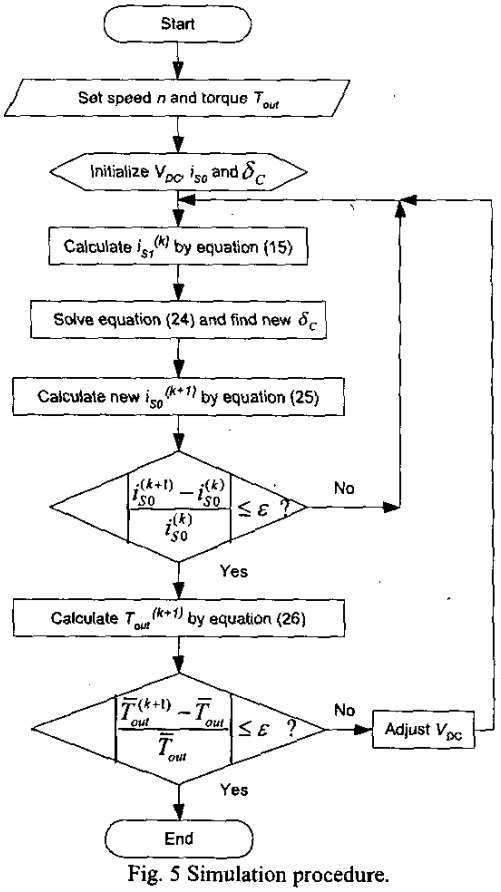

Fig. 5 Simulation procedure.

TABLE III
VALUES OF KEY VARIABLES IN STEADY-STATE SIMULATION

Variables	n	T_{out}	V_{DC}	δ_C	i_{S0}	i_{S1}
Units	(rpm)	(mNm)	(V)	(deg.)	(A)	(A)
Initial value	5400	1.768	7.914	0.0	0.133	
Convergence	5400	1.768	8.798	7.55	0.126	0.197

model is satisfied. Comparing with other approaches, the model is also accurate during computation time as all the equations used are analytic and not complicated in their formats.

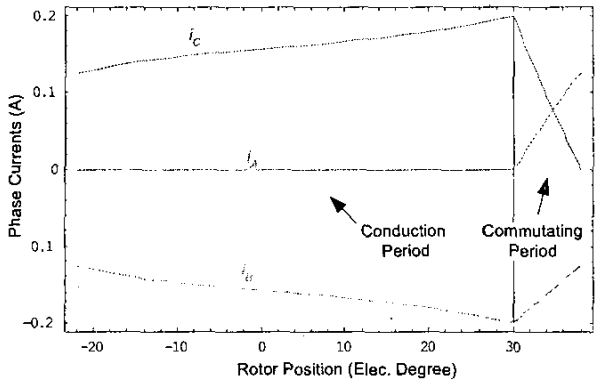

(a) Three phase currents

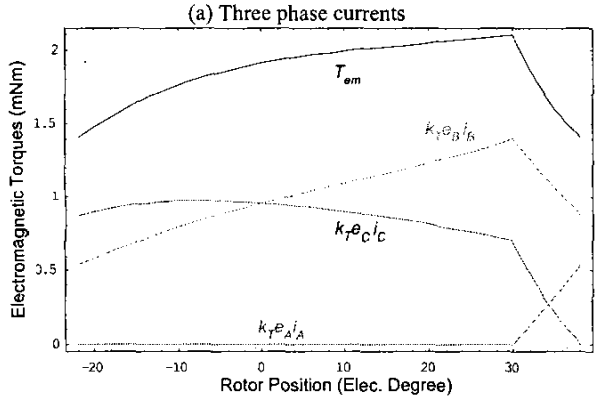

(b) Torques

Fig. 6. Calculating results of one basic operation cycle.

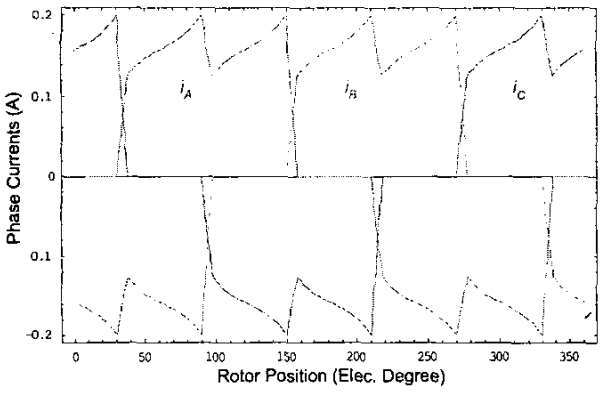

Fig. 7 (a) Calculated three phase currents of a whole electric cycle.

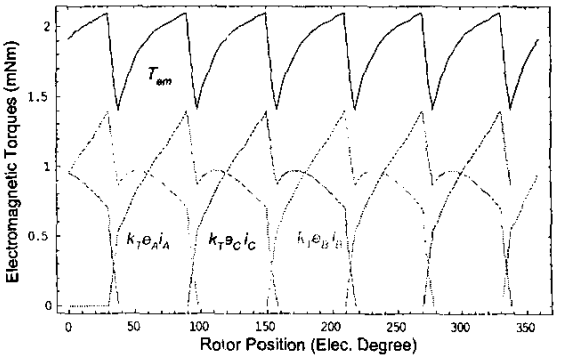

Fig. 7(b). Calculation torques of a whole electric cycle.

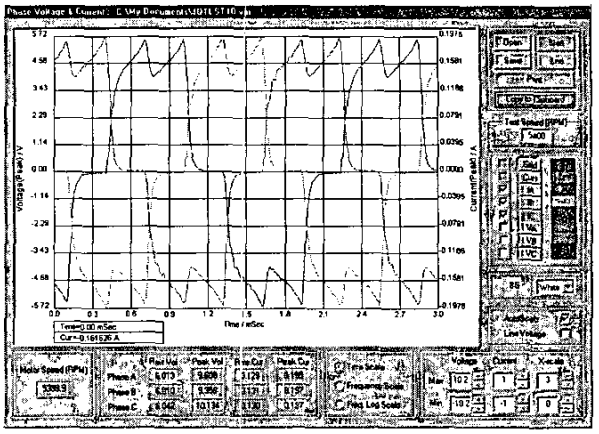

Fig. 8. Measured currents at the same operation status.

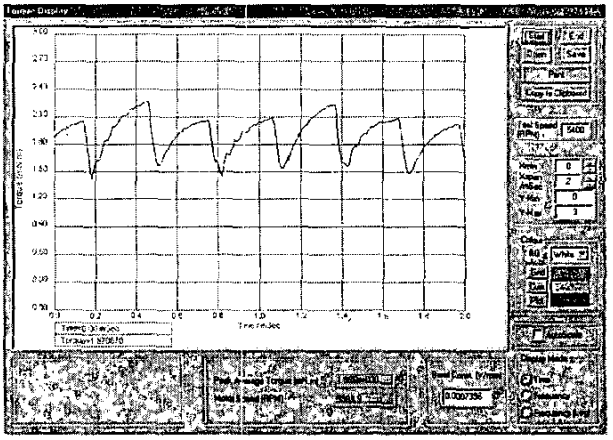

Fig. 9. Measured torque at the same operation status.

IV. CALCULATION OF TORQUE RIPPLE AND EFFICIENCY

The speed stability and efficiency of spindle motors are two important characteristics to HDDs. To improve the speed stability and reduce the speed jitter, the torque ripples are required to be as small as possible. Now, there are two methods to describe the torque ripples. One is using Fourier

series and another is calculating the ratio of peak-to-peak value to the mean value. In this paper, the latter is used to simplify the analysis and is defined as:

$$k_T = \frac{\hat{T}_{em} - \check{T}_{em}}{\bar{T}_{em}} \times 100\%, \tag{28}$$

where $\hat{T}_{em}$ and $\check{T}_{em}$ are maximum and minimum values of electromagnetic torque in (4).

According to the calculated results shown in Fig. 7(b), it can be seen that the maximum and minimum torques happen at the beginning and end of the commutating period, respectively. They are 2.069 mNm and 1.412 mNm in the case of Fig. 7 and the torque ripple ratio is high up to 35%.

The spindle motor in a HDD is always running at the set constant speed after it spins up. It is the major energy-consuming component in HDDs. Therefore, the efficiency of the spin system, including both spindle motor and its inverter, should be as high as possible. For the spindle motor and its inverter, the efficiency can be defined as:

$$\begin{aligned}\eta &= \frac{P_{out}}{P_{out} + p_f + p_{Cu} + p_{iron} + p_{inverter}} \times 100\% \\ &= \frac{\omega_r T_{out}}{\omega_r (T_{out} + T_f) + p_p (p_{Cu} + p_{iron} + p_{inverter})} \times 100\%,\end{aligned} \tag{29}$$

where P_{out} is the output power, p_{Cu} is the stator windings copper loss, $p_{inverter}$ is the power loss on MOSFETs and their diodes, p_{iron} is the core loss, and p_f is the friction loss or the mechanic loss of the spindle motor excluding the windage loss of platters. The core loss and friction loss of HDD spindle motors depend only on the operating speed and are less influenced by the operating currents. They are difficult to be calculated even though numerical methods, e.g., finite element method. In the most of cases, they are obtained through experiments. In the example shown in Table II, their measured values are 0.091 and 0.062 Watts, respectively. The copper loss and inverter loss can be determined only through winding currents. They are:

$$p_{Cu} = R\frac{3}{\pi}\left[\int_{\frac{\pi}{6}+\delta_C}^{\frac{\pi}{6}} 2i_S(\theta)^2 d\theta + \int_{\frac{\pi}{6}}^{\frac{\pi}{6}+\delta_C} [i_A(\theta)^2 + i_B(\theta)^2 + i_C(\theta)^2] d\theta\right] \tag{30}$$

$$\begin{aligned}p_{inverter} &= \frac{3}{\pi}\int_{\frac{\pi}{6}+\delta_C}^{\frac{\pi}{6}} 2r_{DS} i_S(\theta)^2 d\theta \\ &+ \frac{3}{\pi}\int_{\frac{\pi}{6}}^{\frac{\pi}{6}+\delta_C} [r_{DS} i_A(\theta)^2 + r_{DS} i_B(\theta)^2 + i_C(\theta) V_F] d\theta\end{aligned} \tag{31}$$

It should be pointed out that the inverter loss should include the switch-on and switch-off transient losses of MOSFETs and their anti-parallel freewheel diodes. But they are neglected in (31) because the applied MOSFEs and their diodes in this paper can switch on or off in 20 nanoseconds and the correspondent losses are very small. In the example shown in Table II, the copper loss is 0.15 Watts and the inverter loss is 0.11 Watts. Therefore, the system efficiency is 70.6%. It should be noted that the inverter loss is obvious. The parameters of the inverter definitely affect both the current waveforms and the torque ripples as well as system efficiency.

V. CONCLUSIONS

BLDC spindle motors used in hard disk drives are sensorless PM motors and have sinusoidal back EMFs. Analyzing such kind of motors operating in high speed operation is difficult as the transient phenomenon of both the motor and inverter must be considered in the computation. In this paper, a mathematical model is developed for the high speed sensorless PM BLDC motor analysis. The performance of spindle motor running at high speeds can be calculated effectively and fast by using the suggested model, and both the characteristics of motor and the inverter's switches are taken into account. The analysis shows that, the power consuming in the transient commutation period take a quite big ratio of the total power and cannot be neglected in the analysis. The test results also confirm the simulation results.

The computation results show that the electromagnetic torque generated by normal BLDC drive mode is a pulsating torque and its torque ripple ratio can be high up to 35%. The ripples are mainly due to the commutation phenomena, and they are not expected in HDD operation as they cause vibration and acoustic noise. The presented motor model can predict the performances of motor and drive system accurately, and some optimal control methods can thus be developed by using the suggested model. We will use other papers to introduce our research results in this area.

VI. REFERENCES

[1] Y. Miura, "Hard Disk Drive Technology: Past, Present and Future," In *Digest of the Asia-Pacific Magnetic Recording Conference 2002*, 0-7803-7509-2, pp.AK1-01.

[2] T.S. Low et al, "Identity Control for Spindle Motors in Hard-Disk Drives," *IEEE Trans. on Magnetics*, vol. 31, no. 6, Nov. 1995, pp.3117-3119.

[3] S.K. Safi et al, "Analysis and simulation of the high-speed torque performance of brushless DC motor drives", *IEE Proc.-Electr. Power Appli.*, vol. 142, no.3, May 1995, pp.191-200.

[4] H. Zeroug et al, "Analysis of Torque Ripple in BDCM," *IEEE Trans. on Magnetics*, vol. 38, no. 2, March 2002, pp.1293-1296.